# Molecular Force Field for Ionic Liquids III: Imidazolium, Pyridinium, and Phosphonium Cations; Chloride, Bromide, and Dicyanamide Anions

**José N. Canongia Lopes*,† and Agílio A. H. Pádua*,‡**

*Centro de Química Estrutural, Lisboa, Portugal/Instituto de Tecnologia Química e Bioquímica, Oeiras, Portugal and Laboratoire de Thermodynamique des Solutions et des Polymères, Université Blaise Pascal Clermont-Ferrand/CNRS, France*

*Received: June 22, 2006; In Final Form: July 31, 2006*

This is the third set of parameters of a force field for the molecular simulation of ionic liquids, developed within the spirit of the OPLS-AA model and thus oriented toward the calculation of equilibrium thermodynamic and structural properties. The parameter sets reported here concern the cations alkylimidazolium, tetra-alkylphosphonium, and *N*-alkylpyridinium, and the anions chloride, bromide, and dicyanamide. The force field is built in a stepwise manner that allows the construction of models for an entire family of cations, with alkyl side chains of different length, for example. Due to the transferability of the present force field, the ions studied here can be combined with those reported in our two previous publications to create a large variety of ionic liquids that can be studied by molecular simulation. The parameters reported were obtained through different series of ab initio calculations concerning the geometry, force constants, torsion energy profiles, and electrostatic charge distributions of the ions under study. Validation of the force field consisted of comparison with experimental crystal structure and liquid density data.

## Introduction

In two previous articles,[1,2] we presented a systematic molecular force field for the simulation of ionic liquids within the framework of statistical mechanics of fluid phases. In the present report, we extend the scope of that force field to encompass other cations and anions that became common as constituents of ionic liquids of the so-called second or third generation, as well as other more traditional cations not included in our earlier work. The cations studied here include alkylimidazolium—unlike the previously modeled imidazolium cation derivatives, this is a protic cation with a hydrogen atom directly linked to one of the nitrogens of the ring—tetra-alkylphosphonium, and *N*-alkylpyridinium. As far as anions are concerned, the present study addresses chloride, bromide, and dicyanamide anions. The chloride anion was studied in the first article concerning this force field, but the corresponding parameters were not reported correctly in Table 4 of ref 1; the present values will serve as an erratum to that reference. The ions under discussion as well as the nomenclature adopted throughout this article are presented in Chart 1. It is important to stress that some of these ions are already part of other molecular modeling studies—for instance equilibrium and transport properties of *N*-alkylpyridinium-based ionic liquids have been recently estimated by molecular dynamics (MD).[3] The objective of the present study is not to model only "new" ions but rather to complete in a consistent way the force field being developed in our previous publications.

The development of the present force field is based on the same kind of assumptions and follows the same strategy discussed in our previous articles, in other words, it is a force field that expands the OPLS-AA force field,[4] with particular emphasis on compatibility and transferability of parameters within families of ionic liquids (ILs). A special attention is placed upon the evaluation of unknown parameters such as those corresponding to the torsional barriers of articulated molecules or to the electrostatic charge distributions within ions.

The potential function used in this work has the general form

$$u_{\alpha\beta} = \sum_{ij}^{\text{bonds}} \frac{k_{r,ij}}{2}(r_{ij} - r_{0,ij})^2 + \sum_{ijk}^{\text{angles}} \frac{k_{\theta,ijk}}{2}(\theta_{ijk} - \theta_{0,ijk})^2 + \sum_{ijkl}^{\text{dihedrals}} \sum_{m=1}^{4} \frac{V_{m,ijkl}}{2}[1 + (-1)^m \cos(m\,\varphi_{ijkl})] + \sum_{i}\sum_{j\neq i}^{'} \left\{ 4\epsilon_{ij}\left[\left(\frac{\sigma_{ij}}{r_{ij}}\right)^{12} - \left(\frac{\sigma_{ij}}{r_{ij}}\right)^{6}\right] + \frac{1}{4\pi\epsilon_0}\frac{q_i q_j}{r_{ij}} \right\} \quad (1)$$

where we see the traditional decomposition of the potential energy into covalent bonds, valence angles, torsion dihedral angles, and atom−atom pairwise repulsive, dispersive, and electrostatic interactions. The repulsive and dispersive terms are described by the Lennard-Jones 12-6 potential. Together with the Coulombic interactions, given by point charges, they act between sites in different molecules but also between sites within the same molecule separated by three or more bonds. For sites of a same molecule separated by exactly three bonds, a scale factor of 0.5 is introduced into the Lennard-Jones and Coulombic interactions. The function in eq 1 is slightly different from the OPLS-AA convention since in our case the bonded interactions (bonds and angles) described by harmonic potentials have their force constants divided by a factor of 2 (in the OPLS-AA/

* To whom correspondence should be addressed. E-mail: jnlopes@ist.utl.pt; agilio.padua@univ-bpclermont.fr.
† Portugal/Instituto de Tecnologica Química e Bioquímica.
‡ Université Blaise Pascal Clermont-Ferrand/CNRS.

10.1021/jp063901o CCC: $33.50 
Published on Web 09/12/2006

**CHART 1: Adopted Nomenclature for the Interaction Sites of Alkylimidazolium ($C_n$im), Tetra-alkylphosphonium ($P_{i\,j\,k\,l}$), *N*-alkylpyridinium ($C_n$py), and Dicyanamide (dca) Ions**

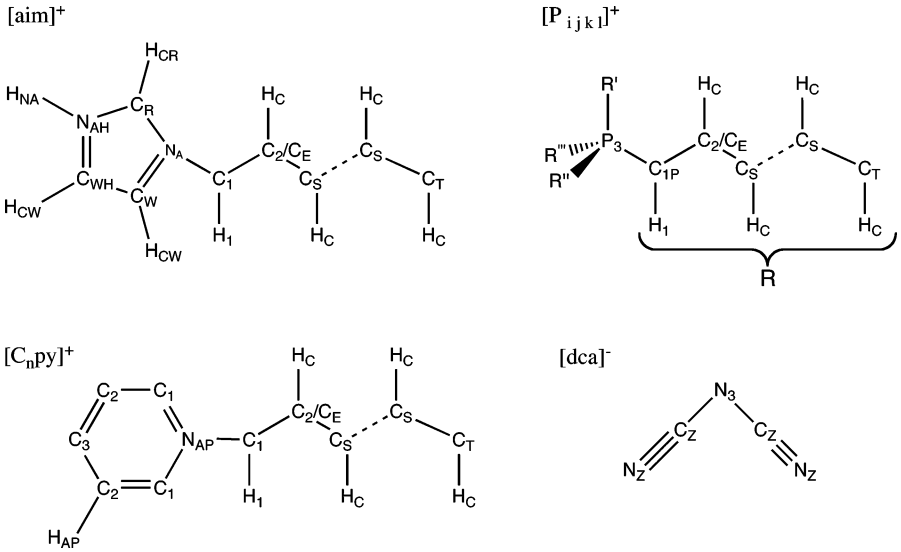


AMBER function,[4,5] only the coefficients of the dihedral cosine series are divided by two). Therefore, all the bond and angle force constants reported here must be divided by two to obtain true OPLS-AA values.

**Force-field Development.** In Table 1, we give our set of parameters for the cations and anions under discussion. The parameters in normal script were taken directly from the OPLS-AA force field or adapted from previous parametrizations of similar ILs within the OPLS framework[1,2] while those in bold are the result of ab initio and MD calculations performed in the present study. For comparison purposes, X-ray diffraction data (RX) is also included in the table. The details of the parametrization procedure for each class of interaction are discussed in the following subsections, for each kind of cation and anion. A complete parameter set can be found as Supporting Information, where all of the families of ILs considered in the present and in our previous reports are included.

**Bond and Angle Parametrization.** Parameters describing covalent bonds and valence angles belong to classes of interaction that are described for a wide variety of chemical structures in the OPLS-AA/AMBER force field. They are also generally easy to transfer, although this does not mean that transferability can be assumed as such. In other words, one must always compare the parameters to be transferred from literature-based molecular residues with available experimental results such as X-ray diffraction data for the target molecules (cf. Table 1). Our force-field model is designed to study equilibrium thermodynamic properties in condensed phases, and this kind of property is not very sensitive to certain intramolecular features that have fast time scales, such as bond stretching and angle bending. (Some other force fields are aimed at describing vibrational modes and require very accurate force constants; this would be the domain of "molecular mechanics", rather than that of "molecular simulation" of condensed phases, which is ours.) Generally, for our purpose, both bond and angle force constants are easier to transfer than the equilibrium distance and angle parameters, since the last two affect the geometry and conformations of the molecules, which are important for our applications.

In cases where direct transfer from the OPLS-AA/AMBER force field was not possible, ab initio calculations (geometry optimizations at the RHF level with the 6-31G(d) basis set using Gaussian[16]) were performed to estimate the missing equilibrium distances and angles. Frequency calculations were performed ab initio to obtain stretching and bending force constants in cases where these were missing. Sometimes, ill-conditioned matrices when converting normal modes into internal modes render these calculations ineffective, and whenever this occurred, the correlation[17] by Halgren was used to assign the corresponding angle-bending force constants.

For the alkylimidazolium cation, the most relevant observation when analyzing the results of our calculations is that the imidazolium ring retains its geometrical symmetry despite the asymmetrical charge distribution between the two nitrogen atoms. This means that the bond and angle parameters defined previously for the dialkyl-imidazolium cations could be retained. The only exception is the NAH−HN distance (1.01 Å) and the CWH/CRH−NAH−HN angles that were estimated ab initio and confirmed against X-ray data or existing OPLS-AA values.[6] The force constants were taken directly from the OPLS-AA force field.

In the case of *N*-alkylpyridinium cations, the work of Jorgensen and coauthors contained some of the required parameters.[8] Although in their case the pyridinium cations were part of larger macrocyclic molecules, the average bonds and angles from OPLS-AA compared favorably both with X-ray data and with the ab initio results obtained during this work (cf. Table 1). The missing parameters were calculated ab initio and agree with experimental diffraction data.

The existing OPLS-AA bond parameters for tetra-alkylphosphonium cations[10] compared well both with experimental X-ray data and with our own ab initio calculations and were retained. Equilibrium angles were evaluated ab initio, and the corresponding force constants were estimated using the Halgren correlation. The former parameters compared well with X-ray results (cf. Table 1).

For the dicyanamide anion, the OPLS-AA databases only had data corresponding to the bond between carbon and nitrogen in the nitrile group.[14] All other bond and angle parameters were calculated ab initio. When performing molecular dynamics simulations of liquid phases, to avoid convergence problems related to the N3−CZ−NZ angle being close to 180°, this anion was modeled as a rigid unit (the bond and angle and dihedral constants were not taken into account).

**Dihedral Angle Parametrization.** To obtain the dihedral parameters for the cations under discussion, we used a procedure

**TABLE 1: Force Field Parameters for Ionic Liquids Containing Alkylimidazolium, *N*-alkylpyridinium, Tetra-alkylphosphonium, Bromide, Chloride, and Dicyanamide Ions**

*N*-alkylimidazolium, $[C_n im]^+$ (OPLS from ref 6, X-ray diffraction, XR, data from ref 7)

| atoms | $q$ (e) | $\epsilon$ (kJ mol$^{-1}$) | $\sigma$ (Å) | bonds | $r_0$ (Å) | $k_r$ (kJ mol$^{-1}$ Å$^{-2}$) | $r_0$ (Å) XR |
|---|---|---|---|---|---|---|---|
| CRH | **0.00** | 0.293 | 3.55 | NAH−HNA | **1.01** | | |
| NAH | **−0.21** | 0.711 | 3.25 | angles | $\theta_0$ (deg) | $k_\theta$ (kJ mol$^{-1}$ rad$^{-2}$) | $\theta_0$ (deg) XR |
| CWH | **−0.03** | 0.293 | 3.55 | CRH−NAH−HNA | **125.4** | 293 | 125.0 |
| HNA | **0.37** | 0.000 | 0.00 | CWH−NAH−HNA | **126.6** | 293 | 126.0 |

*N*-alkylpyridinium, $[C_n py]^+$ (OPLS from ref 8, XR data from ref 9)

| atoms | $q$ (e) | $\epsilon$ (kJ mol$^{-1}$) | $\sigma$ (Å) | angles | $\theta_0$ (deg) | $k_\theta$ (kJ mol$^{-1}$ rad$^{-2}$) | $\theta_0$ (deg) XR |
|---|---|---|---|---|---|---|---|
| NAP | **0.15** | 0.711 | 3.25 | CA1−NAP−CA1 | **120.4** | 586 | 120.4 |
| CA1 | **0.00** | 0.293 | 3.55 | CA1−NAP−C1 | **119.8** | 586 | 119.8 |
| CA2 | **−0.07** | 0.293 | 3.55 | NAP−CA1−CA2 | **120.0** | 586 | 120.4 |
| CA3 | **0.02** | 0.293 | 3.55 | CA*−CA*−CA* | **120.0** | 586 | 119.7 |
| HAP | **0.15** | 0.126 | 2.42 | NAP−CA1−HAP | **120.0** | 293 | |
| bonds | $r_{0,b}$ (Å) | $k_{r,b}$ (kJ mol$^{-1}$ Å$^{-2}$) | $r_{0,b}$ (Å) RX | CA*−CA*−HAP | **120.0** | 293 | |
| NAP−CA1 | **1.34** | 4042 | 1.35 | dihedrals | | $V_2$ (kJ mol$^{-1}$) | $V_4$ (kJ mol$^{-1}$) |
| CA*−CA* | **1.38** | 3925 | 1.37 | CA*−NAP−C1−H1 | | **0.000** | **0.000** |
| NAP−CA1 | **1.34** | 4042 | 1.35 | CA*−NAP−C1−C2/E | | **1.092** | **0.793** |
| CA*−CA* | **1.38** | 3925 | 1.37 | | | | |

tetra-alkylphosphonium, $[P_{i\,j\,k\,l}]^+$ (OPLS from ref 10, XR data from ref 11)

| atoms | $q$ (e) | $\epsilon$ (kJ mol$^{-1}$) | $\sigma$ (Å) | angles | $\theta_0$ (deg) | $k_\theta$ (kJ mol$^{-1}$ rad$^{-2}$) | $\theta_0$ (deg) XR |
|---|---|---|---|---|---|---|---|
| P3 | **0.68** | 0.837 | 3.74 | P3−C1P−H1 | **110.1** | **390** | 108.7 |
| C1P | **−0.31** | 0.276 | 3.50 | dihedrals | $V_1$ (kJ mol$^{-1}$) | $V_2$ (kJ mol$^{-1}$) | $V_3$ (kJ mol$^{-1}$) |
| bonds | $r_0$ (Å) | $k_r$ (kJ mol$^{-1}$ Å$^{-2}$) | $r_{0,b}$ (Å) RX | C1P−P3−C1P−H1 | **0** | **0** | **0.927** |
| P3−C1P | **1.81** | 1775 | 1.8 | C1P−P3−C1P−C2 | **0** | **0** | **1.133** |
| angles | $\theta_0$ (deg) | $k_\theta$ (kJ mol$^{-1}$ rad$^{-2}$) | $\theta_{0,a}$ (deg) RX | P3−C1P−C2−HC | **0** | **0** | **0.465** |
| C1P−P3−C1P | **109.5** | **608** | 109.5 | P3−C1P−C2−CS/T | **−3.248** | **0.988** | **−0.715** |
| P3−C1P−C2 | **115.2** | **509** | 114.3 | | | | |

halide, $Cl^-$, $Br^-$ (LJ parameters based on refs 12 and 13)

| atom | $q$ (e) | $\epsilon$ (kJ mol$^{-1}$) | $\sigma$ (Å) | atom | $q$ (e) | $\epsilon$ (kJ mol$^{-1}$) | $\sigma$ (Å) |
|---|---|---|---|---|---|---|---|
| Cl | **−1.00** | **0.83** | **3.65** | Br | **−1.00** | **0.86** | **3.97** |

dicyanamide, $[dca]^-$ (OPLS from ref 14, XR data from ref 15)

| atoms | $q$ (e) | $\epsilon$ (kJ/mol) | $\sigma$ (Å) | angles | $\theta_0$ (deg) | $k_\theta$ (kJ mol$^{-1}$ rad$^{-2}$) | $\theta_0$ (deg) XR |
|---|---|---|---|---|---|---|---|
| N3 | **−0.76** | 0.711 | 3.25 | CZ−N3−CZ | **118.5** | **362** | 120.7 |
| CZ | **0.64** | 0.276 | 3.30 | N3−CZ−NZ | **175.2** | **425** | 173.3 |
| NZ | **−0.76** | 0.711 | 3.20 | dihedrals | $V_1$ (kJ mol$^{-1}$) | $V_2$ (kJ mol$^{-1}$) | $V_3$ (kJ mol$^{-1}$) |
| bonds | $r_0$ (Å) | $k_r$ (kJ mol$^{-1}$ Å$^{-2}$) | $r_0$ (Å) RX | CZ−N3−CZ−NZ | **4.08** | **0** | **0** |
| N3−CZ | **1.31** | **4206** | 1.31 | | | | |
| CZ−NZ | **1.15** | **7746** | 1.15 | | | | |

similar to the one used in previous works.[1,2] To separate the contributions from bonded and nonbonded interactions to the torsional energy profile, several ab initio calculations using constrained configurations of the dihedral under scrutiny were implemented. These consist of geometry optimizations at the RHF/6-31G(d) level followed by energy calculation at the MP2/cc-pVTZ(-f) level. These were followed by molecular dynamics runs (using the DL_POLY package[18]) under similar constraints and with the parameters of the selected dihedral set to zero. From the obtained torsion energy profiles, one can then fit the appropriate function (generally a cosine series) that will reproduce the ab initio results in a MD run.

For the alkylimidazolium cations, such a procedure was used to check the hypothesis that the parameter set previously obtained for the dialkylimidazolium cations[1] was transferable to these new cations. Such a possibility became apparent when it was observed that the alkyl residues and the atoms to which they were attached in the aromatic rings had very similar geometrical (bonds, angles) and nonbonded interaction (point charges, dispersion, repulsion) parameters.

In the dihedral angle CRH−NA-C1−H1 of alkylimidazolium, the height of the torsion barrier at 0° calculated ab initio was 1.9 kJ mol$^{-1}$, comparable to the value of 2.2 kJ mol$^{-1}$ obtained for 1,3-dialkylimidazolium cations (cf. Figure 3 of ref 1). Additional ab initio calculations yielded a torsion energy profile for the CRH−NA-C1−C2 dihedral with a maximum at 0° of 4.7 kJ mol$^{-1}$ and a local minimum at 180° of 1.9 kJ mol$^{-1}$ that compare very well with values of 4.4 and 1.7 kJ mol$^{-1}$, respectively, for the dialkylated species (cf. again Figure 3 of ref 1). Such small differences allowed us to transfer the dihedral parametrization from 1,3-dialkylimidazolium cations to the monoalkylated imidazolium cations.

The alkylpyridinium ring is more symmetrical than the corresponding imidazolium-based cations, which means that there are fewer different dihedrals to be parametrized. As in the case of imidazolium cations, the dihedrals involving atoms that belong to the ring or are directly attached to it were taken from the AMBER force field.[5] The same applies to dihedrals that involve only carbon or hydrogen atoms of the aliphatic chain. Therefore, the parameters to be obtained here are those of the junction between the aromatic ring and the aliphatic chain, namely, the CA1−NAP−C1−H1, CA1−NAP−C1−C2/CE, NAP−C1−C2/CE−HC, and NAP−C1−C2−CS/CT dihedrals. Since the electrostatic charges of the atoms involved in the last two dihedrals are similar to those of the imidazolium cations (cf. Table 1), and the geometry around the two central atoms is

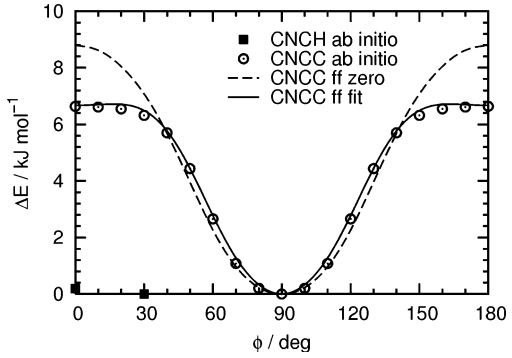


**Figure 1.** Torsion profile for two dihedral angles around the NAP−C1 bond in the *N*-alkylpyridinium molecule.

also the same (two $sp^3$ aliphatic carbons), it was also possible in these two cases to use the dialkylimidazolium parameters. For the two remaining dihedrals, the torsional energy profiles were explicitly calculated and are shown in Figure 1.

The results show that the rotation of the methyl group around the NAP−C1 bond in *N*-methylimidazolium is almost free, whereas the C1−C2 bond in longer alkyl chains adopts an orientation perpendicular to the aromatic ring. Accordingly, the dihedral parameters of the former dihedral angle were set to zero while those of the latter were fitted to a cosine series with non-null terms in $V_2$ and $V_4$. The term in $V_4$ is necessary to reproduce the flatness of the profile near the top of the rotational barrier.

For phosphonium cations, we developed a new set of parameters to describe the C−P−C−H, C−P−C−C, P−C−C−H, and P−C−C−C dihedrals. The results are condensed in Figure 2. Three of the dihedral angles (C−P−C−H, C−P−C−C, and P−C−C−H) exhibit a simple torsion profile with a 120° period and an energy barrier around 10 kJ $mol^{-1}$ that reflects the $sp^3$ character of the central atom and the constrained nature of the four carbon atoms attached to the phosphorus atom. The torsion profile of the P−C−C−C dihedral in longer alkyl chains is more complex and reflects the more articulated character of those chains. It is seen that the energy profile can be reproduced almost exclusively by nonbonded interactions (compare the dashed line and the open triangles in the lower plot of Figure 2). This means that, in phosphonium cations containing several long alkyl chains, the conformational space available to the molecules will be determined by this type of interaction. It also means that the nonbonded parameters adopted for the present force field were able to reproduce the ab initio results, which lends some degree of confidence to the approximations performed while trying to generalize the atomic charges for the tetra-alkylphosphonium cation family.

The two equivalent dihedral angles of the dicyanamide anion were parametrized in a similar manner, by separating the contribution from nonbonded interactions from the overall interactions calculated ab initio. The minimum in the dihedral energy profile corresponds to the outward-bended conformation of Chart 2a, which is 12 kJ $mol^{-1}$ more stable than the inward-bending conformation of Chart 2b and 6 kJ $mol^{-1}$ more stable than the inward-outward conformation of Chart 2c. Please note that all conformations depicted in Chart 2 are planar; the "inward" and "outward" designations refer to the position of the CN terminal bonds relative to the CNC central angle. The values found indicate that intramolecular interactions are additive. The contribution of the nonbonded interactions in the last two conformations is ca. 4 and 2 kJ $mol^{-1}$, respectively, with the remaining being described by the dihedral cosine series.

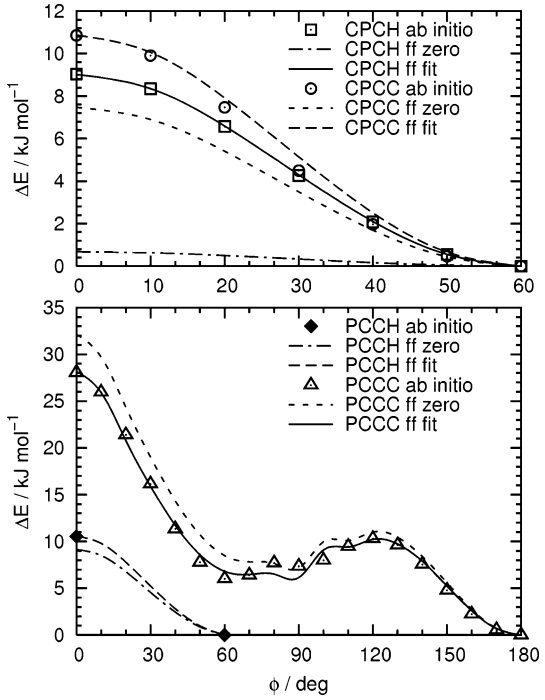


**Figure 2.** Torsion profile for the dihedral angles around the NAP−C1 bond (top plot) and the C1−C2/E bond (bottom plot) in the tetra-alkylphosphonium cation.

**CHART 2: Conformers of the Dicyanamide Anion**

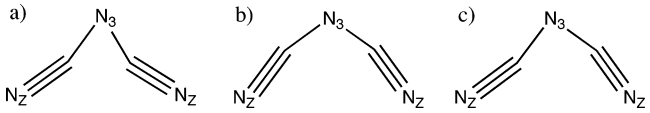


**Repulsive and Dispersive Terms.** The OPLS-AA force field comprises repulsion−dispersion terms represented by the Lennard-Jones (12-6) potential function. The Lennard-Jones parameters for each type of atom in the cations were taken from the OPLS-AA model of heterocyclic aromatic rings (imidazolium and pyridinium cations) and tetra-alkylphosphorus compounds. For the bromide anion, the Lennard-Jones parameters were obtained from a fit to a Born−Higgins−Mayer potential function, originally developed to describe the interactions of these anions in molten salts[12] and bromoapatite crystals.[13] Finally, the dicyanamide anion parameters were taken from the OPLS-AA force field, namely, the values used for nitrile residues in other organic molecules and for the central nitrogen of the bistriflamide anion $[(CF_3SO_2)_2N]^-$. The repulsive−dispersive unlike interactions between atoms of different types were computed using combining rules with geometric means for both $\sigma$ and $\epsilon$.

**Coulombic Charges.** The partial charges on each atom were calculated from the electron density obtained by ab initio calculation, using an electrostatic surface potential methodology (electronic density and energy calculation at the MP2 level with a cc-pVTZ(-f) basis set and point charge fitting using the CHelpG methodology[19]). Since one of the objectives of the present force field is the endorsement of parameter transfer within families of ILs, the point charges attributed to the various molecular residues were subjected to different degrees of approximation to find general trends that could then be applied along an entire series of analogous ILs.

In the case of the monoalkylated imidazolium cation, only the charges referring to the NAH and HNA atoms had to be calculated and those of the atoms adjoining NAH (CW and CR)

had to be re-parametrized (as CWH and CRH). All other charges were transferred from the dialkylimidazolium parametrization.

For *N*-alkylpyridinium, only the aromatic ring (the six atoms of the ring plus the five hydrogen atoms bonded to it) had to be parametrized. The charges on the nitrogen atom and on the alkyl chain attached to it (including the two carbon atoms closest to the ring, C1 and C2) could retain the same charges used in the parametrization of the alkylimidazolium cations. To reach such a generalization, the ab initio charge distributions of *N*-methyl to *N*-butylpyridinium cations were calculated and compared with the charge distributions in the alkyl chains of alkylimidazolium cations. The results showed that there is some variability in the charge distribution along the chain as it increases in length: typically, one can find fluctuations around $q/e = \pm 0.1$ (probably due to hyper-conjugation effects or even to spurious effects introduced by the charge attribution algorithm itself). But if one considers the total charge assigned to each methylene ($-CH_2-$) or methyl group ($-CH_3$) and compares that with the situation along the alkyl chain of an alkylimidazolium, the differences can be accommodated in a unified set of parameters.

The situation in the tetra-alkylphosphonium cations is similar to the one just discussed: although the parametrization of C1 (the alkyl chain carbon adjoining the phosphorus atom) had to be changed, the rest of the charges in the alkyl chains could be transferred from the alkylimidazolium cations. To reach this conclusion (and also to establish the charge on the phosphorus atom), four ab initio runs, in tetramethyl-, ethyltrimethyl-, propyltrimethyl-, and butyltrimethyl-phopshonium cations, were performed. The results exhibited some charge distribution fluctuations, but these could be adjusted to fit a general set of parameters that is similar to the alkylimidazolium and OPLS-AA values for alkyl atoms other than C1.

The charges in the dicyanamide anion were obtained ab initio. The results show that the three nitrogen atoms, albeit their different nature, all bear the same value for their point charges.

**Validation.** As in the two previous articles concerning the present force field[1,2] and since most of the currently available experimental results concerning equilibrium thermodynamic properties of ILs are related to their volumetric properties, we decided to continue to test the performance of the proposed force field by estimating the molar densities of ILs containing at least one of the cations or anions under discussion, in both the crystalline and liquid phases.

**Crystal Structures.** Three IL crystalline structures containing cations of the *N*-alkylpyridinium or tetra-alkylphosphonium families and the dicyanamide or bromide anions were selected from the Cambridge Structural Database, CSD.[20] No crystalline structure containing the 1-methylimidazolium cation was found in the database: the reported crystallographic data for 1-methylimidazolium[21] was incomplete. The crystalline structures studied by MD simulation were those of *N*-butylpyridinium chloride,[9] $[C_4py][Cl]$, tetradecylphosphonium bromide, $[P_{10\ 10\ 10\ 10}][Br]$,[11] and tetramethylammonium dicyanamide, $[N_{1\ 1\ 1\ 1}][dca]$.[15] These choices reflect on one hand the small amount of structures containing the desired cations and anions but also the fact that in these compounds they are all paired with counterions already parametrized by the present force field, namely, tetra-alkylammonium,[2] chloride,[2] and tetrafluoroborate.[2]

The objective of the simulations is to test the performance of the force field in predicting both the crystal density and its structural properties such as the dimensions and director angles of the crystalline unit cell. The adequacy of the test was checked by allowing slightly modified crystal structures to evolve to the reported experimental structure (a similar situation was previously reported[2]). With the tetramethylammonium dicyanamide crystal, the simulation was also performed at a higher temperature, where the solid phase is known to exist as a "plastic" crystal phase[15] and the reported density was also predicted correctly (within 1.5% accuracy, cf. below). In fact, tetramethylammonium dicyanamide is an ambient-temperature plastic electrolyte material: a solid where one or more species within the crystalline lattice can undergo some kind of rotational motion.

The simulation boxes and initial configurations were set by taking into account the dimensions and occupancy of the unit cells of each crystalline structure given by the CSD data. Because the dimensions of the unit cells of most of the crystals are too small to accommodate a sufficiently large cutoff distance, several cells were stacked together to form a sufficiently large and well-proportioned simulation box, with cutoff distances larger than 10 Å. Long-range corrections were applied to the Lennard-Jones interactions beyond those distances, and the Ewald method was implemented to take into account the long-range character of the electrostatic interactions. Since the overall size of the simulation box is defined by the dimensions of the unit cell of each crystal, simulations with different box sizes and cutoff distances (up to 18 Å) were run to check that the dimensions of the simulation box and the cutoff were sufficiently large to make any finite-size effects negligible. The simulations were performed using a Nosé-Hoover thermostat coupled with an anisotropic Hoover barostat that allowed the simulation box to change volume and shape under constant (*N, p, T*) conditions. The temperatures were fixed to match those used during the crystallographic experiments, and the pressure was set to a null value. All runs were allowed to equilibrate for a period of 0.2 ns, followed by production times of at least 0.4 ns. These simulation times were found appropriate since the runs are started from a known initial configuration (the experimental equilibrium structure), and it was observed that the relaxation is complete well before the end of the equilibration period. The simulation results for each crystal are given in Table 2. The densities of all crystals are predicted with an accuracy better than 3.4%.

It is important to notice that (i) the deviations are of the same order of magnitude as those obtained by other authors when comparing the performance of their IL models against experimental density data, (ii) the level of agreement is very good considering that the calculations are purely predictive, as all parameters used were either taken as such from the OPLS-AA/AMBER force field or calculated ab initio, none was adjusted to match the kind of experimental data against which comparison is made, and (iii) in some cases experimental IL density results from different sources also exhibit deviations in the 2−4% range.

**Liquid Phase.** Five ILs with known density and containing at least one of the cations or anions under discussion were selected from the literature. These include trihexyl(tetradecyl)-phosphonium chloride and bromide, $[P_{6\ 6\ 6\ 14}][Cl]$ and $[P_{6\ 6\ 6\ 14}][Br]$,[22] *N*-butylpyridinium tetrafluoroborate, $[C_4py][BF_4]$,[23] 1-butyl-3-methylimidazolium dicyanamide, $[C_4mim][dca]$,[24] and 1-methylimidazolium chloride, [mim][Cl].[25]

The ILs containing the large phosphonium cations were simulated by MD in periodic cubic boxes containing 100 pairs of ions, whereas the small 1-methylimidazolium cation was simulated using 300 ionic pairs; all other ionic liquids were represented by 250 pairs. Cutoffs were taken at 16 Å for short-range Lennard-Jones interactions, with appropriate tail correc-

**TABLE 2: Comparison of Simulated Crystal Structures with Experimental Data from the Cambridge Structural Database (CSD)**

| | [$C_4$py][Cl] | [$P_{10\ 10\ 10\ 10}$][Br] | [$N(CH_3)_4$][dca] | |
|---|---|---|---|---|
| CSD code[a] | FAXVEF[9] | XISCUX[11] | ILUYIX [15] | |
| space group | 19 ($P2_12_12_1$) | 15 ($C2/c$) | 61 ($Pbca$) | |
| ion pairs/box | 144 | 16 | 96 | |
| stacked cells | 4 × 3 × 3 | 2 × 2 × 1 | 3 × 2 × 2 | |
| cutoff/Å | 14.5 | 12.5 | 12.5 | |
| $T$/K | 298 | 173 | 123 | 363 |
| ion pairs/cell | 4 | 4 | 8 | |
| $a_{exp}$/Å | 8.095 | 13.671 | 8.6955 (2) | 8.8934 (3) |
| $a_{sim}$/Å | 8.23 (3) | 13.46 (7) | 8.65 (4) | 9.10 (3) |
| $b_{exp}$/Å | 10.621 | 13.823 | 12.3268 (3) | 12.3402 (4) |
| $b_{sim}$/Å | 10.44 (6) | 13.58 (5) | 12.41 (5) | 12.05 (5) |
| $c_{exp}$/Å | 11.419 | 45.948 | 15.3562 (3) | 16.0710 (6) |
| $c_{sim}$/Å | 11.41 (4) | 46.8 (2) | 15.03 (9) | 15.41 (7) |
| $\alpha_{exp}$/(deg) | 90 | 90 | 90 | 90 |
| $\alpha_{sim}$/(deg) | 90.0 (2) | 90.0 (4) | 90.0 (3) | 90.0 (6) |
| $\beta_{exp}$/(deg) | 90 | 90.053 | 90 | 90 |
| $\beta_{sim}$/(deg) | 90.0 (3) | 90.2 (3) | 90 (1) | 90.0 (7) |
| $\gamma_{exp}$/(deg) | 90 | 90 | 90 | 90 |
| $\gamma_{sim}$/(deg) | 90.0 (4) | 90.0 (3) | 90.0 (5) | 90.0 (3) |
| $V_{exp}$/Å$^3$ | 981.77 | 8683.0 | 1646.0 (6) | 1763.7 (6) |
| $V_{sim}$/Å$^3$ | 980.3 (4) | 8562 (34) | 1612 (18) | 1705 (16) |
| $\rho_{exp}$/mol dm$^{-3}$ | 6.765 | 0.7649 | 8.069 | 7.531 |
| $\rho_{sim}$/mol dm$^{-3}$ | **6.77 (2)** | **0.776 (3)** | **8.23 (14)** | **7.78 (13)** |
| $\delta\rho$/% | **+ 0.2** | **+ 1.8** | **+ 2.1** | **+ 3.3** |

[a] The six-letter code is the alias of each crystal in the Cambridge Structural Database.

**TABLE 3: Comparison of Simulated Liquid Densities with Experimental Data**

| | [mim][Cl] | [$C_4$py][$BF_4$] | [$C_4$mim][dca] | [$P_{6\ 6\ 6\ 14}$]Cl] | [$P_{6\ 6\ 6\ 14}$][Br] |
|---|---|---|---|---|---|
| T/K | 353 | 313/293 | 297 | 298 | 298 |
| $\rho_{exp}$/mol dm$^{-3}$ | 9.977[22] | 5.394[23]/5.416[a] | 5.16[24] | 1.69[25,b] | 1.70[25,b] |
| $\rho_{sim}$/mol dm$^{-3}$ | **10.20 (4)** | **5.26 (2)/5.31 (2)** | **5.144** | **1.677 (7)** | **1.663 (9)** |
| $\delta\rho$/% | **+1.2** | **−2.5/−1.9** | **−0.3** | **−0.8** | **−2.2** |

[a] Extrapolated from experimental data. [b] Experimental data only in graphical form.

tions, and the long-range coulombic forces were handled by Ewald sums. Nosé-Hoover thermostats and barostats were activated to maintain temperature and pressure, with time constants of 0.1 and 0.5 ps, respectively.

The equilibration period in the liquid-phase simulation runs is very important. Different approaches were used to ensure that the ergodicity of the simulation was properly attained: Initially, the ions are placed at random in the simulation box, at very low density, and the equilibration starts by a short relaxation of a few picoseconds at 1 K and constant ($N$, $V$, $E$), to allow internal modes to relax. Then, an equilibration period is imposed at the final temperature of the simulation, followed by the activation of the thermostat and barostat. Alternatively, other simulations of the same system were allowed to evolve from initial configurations based on the expanded structure of an analogous ionic crystal. Another method to ensure the ergodicity of the simulation is to perform several temperature annealing cycles or to scramble/unscramble the two components (ions) of the system by switching off/on the electrostatic charges. The equilibration was considered successful only after stable and consistent results over periods of at least 100 ps. The production runs took at least 400 ps and were made in ($N$, $p$, $T$) conditions, under a pressure of 1 bar and at a temperature matching that of a liquid density reported in the literature. Simulation and relevant experimental data are presented in Table 3.

The agreement of simulated densities with experiment could eventually be improved by fine-tuning some of the parameters proceeding case-by-case. In our previous reports on force-field development for ILs, we concluded that it was difficult to attribute the sign of the deviations to a certain cation family or anion and could not devise a strategy to improve the results in a general and transferable manner. We continue to feel that an accuracy of at the worst 3% in liquid densities is reasonable and justified by the generality and transferability of the present model.

**Acknowledgment.** The authors acknowledge support under the cooperation program PICS 3090 between the CNRS (France) and GRICES (Portugal) and access to the national computing centers IDRIS and CINES in France.

**Supporting Information Available:** A table containing the entire parameter set developed within the framework of the present force field (compatible with the OPLS-AA force field) is provided. This material is available free of charge via the Internet at http://pubs.acs.org.

## References and Notes

(1) Canongia Lopes, J. N.; Deschamps, J.; Pádua, A. A. H. *J. Phys. Chem. B* **2004**, *108*, 2038. Canongia Lopes, J. N.; Deschamps, J.; Pádua, A. A. H. *J. Phys. Chem. B* **2004**, *108*, 11250.

(2) Canongia Lopes, J. N.; Pádua, A. A. H. *J. Phys. Chem. B* **2004**, *108*, 16893.

(3) Cadena, C.; Zhao, Q.; Snurr, R. Q.; Maginn, E. J. *J. Phys. Chem. B* **2006**, *110*, 2821.

(4) Jorgensen, W. L.; Maxwell, D. S.; Tirado-Rives, J. *J. Am. Chem. Soc.* **1996**, *118*, 11225. Kaminsky, G.; Jorgensen, W. L. *J. Phys. Chem.* **1996**, *100*, 18010.

(5) Cornell, W.; Cieplak, P.; Bayly, C. I.; Gould, I. R.; Merz, K. M., Jr.; Ferguson, D. M.; Spellmeyer, D. C.; Fox, T.; Caldwell, J. W.; Kollman, P. A. *J. Am. Chem. Soc.* **1995**, *117*, 5179.

(6) McDonald, N. A.; Jorgensen, W. L. *J. Phys. Chem. B* **1998**, *102*, 8049.

(7) Arduengo, A. J., III; Dias, H. V. R.; Harlow, R. L.; Kline, M. *J. Am. Chem. Soc.* **1992**, *114*, 5530.

(8) Jorgensen, W. L.; McDonald, N. A. *J. Mol. Struct. (THEOCHEM)* **1998**, *424*, 145. Kamiski, G. A.; Jorgensen, W. L. *J. Chem. Soc., Perkin Trans. 2* **1999**, 2365.

(9) Ward, D. L.; Rhinebarger, R. R.; Popov, A. I. *Acta Crystallogr., Sect. C: Cryst. Struct. Commun.* **1986**, *42*, 177 1.

(10) Gunsteren W.; Berendsen. H. *GROMOS: GROningen MOlecular Simulation software*. Technology Report, Laboratory of Physical Chemistry, University of Groningen, Groningen, The Netherlands, 1988.

(11) Abdallah, D. J.; Bachman, R. E.; Perlstein, J.; Weiss, R. G. *J. Phys. Chem. B* **1999**, *103*, 9269.
(12) Tosi, M. P.; Fumi, G. *J. Phys. Chem. Solids* **1964**, *25*, 45.
(13) Cruz, F. J. A. L.; Canongia Lopes, J. N.; Calado, J. C. G.; Minas da Piedade, M. E. *J. Phys. Chem. B* **2005**, *109*, 24473.
(14) Price, M. L.; Ostrovsky, D.; Jorgensen, W. L. *J.* Comput. Chem. **2001**, *22*, 1340.
(15) Seeber, A. J.; Forsyth, M.; Forsyth, C. M.; Forsyth, S. A.; Annatb, G.; MacFarlane, D. R. *Phys. Chem. Chem. Phys*. **2003**, *5*, 2692.
(16) Frisch, M. J.; Trucks, G. W.; Schlegel, H. B.; Scuseria, G. E.; Robb, M. A.; Cheeseman, J. R.; Montgomery, J. A., Jr.; Vreven, T.; Kudin, K. N.; Burant, J. C.; Millam, J. M.; Iyengar, S. S.; Tomasi, J.; Barone, V.; Mennucci, B.; Cossi, M.; Scalmani, G.; Rega, N.; Petersson, G. A.; Nakatsuji, H.; Hada, M.; Ehara, M.; Toyota, K.; Fukuda, R.; Hasegawa, J.; Ishida, M.; Nakajima, T.; Honda, Y.; Kitao, O.; Nakai, H.; Klene, M.; Li, X.; Knox, J. E.; Hratchian, H. P.; Cross, J. B.; Bakken, V.; Adamo, C.; Jaramillo, J.; Gomperts, R.; Stratmann, R. E.; Yazyev, O.; Austin, A. J.; Cammi, R.; Pomelli, C.; Ochterski, J. W.; Ayala, P. Y.; Morokuma, K.; Voth, G. A.; Salvador, P.; Dannenberg, J. J.; Zakrzewski, V. G.; Dapprich, S.; Daniels, A. D.; Strain, M. C.; Farkas, O.; Malick, D. K.; Rabuck, A. D.; Raghavachari, K.; Foresman, J. B.; Ortiz, J. V.; Cui, Q.; Baboul, A. G.; Clifford, S.; Cioslowski, J.; Stefanov, B. B.; Liu, G.; Liashenko, A.; Piskorz, P.; Komaromi, I.; Martin, R. L.; Fox, D. J.; Keith, T.; Al-Laham, M. A.; Peng, C. Y.; Nanayakkara, A.; Challacombe, M.; Gill, P. M. W.; Johnson, B.; Chen, W.; Wong, M. W.; Gonzalez, C.; and Pople, J. A. *Gaussian 03*, revision C.05; Gaussian, Inc.: Wallingford, CT, 2004.
(17) Halgren, T. A. *J. Am. Chem. Soc.* **1990**, *112*, 4710.
(18) Smith, W.; Forester, T. R. *The DL_POLY package of molecular simulation routines*, version 2.12; The Council for The Central Laboratory of Research Councils: Daresbury Laboratory, Warrington, U.K., 1999.
(19) Breneman, C. M.: Wiberg, K. B. *J. Comput. Chem*. **1990**, *11*, 361.
(20) Allen,F. H. *Acta Crystallogr. Sect. B: Struct. Sci*. **2002**, *58*, 380.
(21) Wilkes, J. S.; Zaworotko, M. J. *Supramol. Chem.* **1993**, *1*, 191.
(22) Bradaric, C. J.; Downard, A.; Kennedy, C.; Robertson, A. J.; Zhou, Y. *Green Chem.* **2003**, *5*, 143.
(23) Blanchard, L. A.; Gu, Z.; Brennecke, J. F. *J. Phys. Chem. B* **2001**, *105*, 2441.
(24) Fredlake, C. P.; Crosthwaite, J. M.; Hert, D. G.; Aki, S. N. V. K.; Brennecke, J. B. *J. Chem. Eng. Data* **2004**, *49*, 954.
(25) Basionics Portfolio AC75, BASF Aktiengesellschaft, 2005.